International Geotechnical Symposium on Theory and Practice of Earth Reinforcement / Fukuoka Japan / 5-7 October 1988
 ISBN 906191 8200

Role of facing in reinforcing cohesionless soil slopes by means of metal strips

V.Gutierrez
Sumitomo Construction Co., Ltd, Japan
(Formerly: University of Tokyo, Japan)

F.Tatsuoka
Institute of Industrial Science, University of Tokyo, Japan

ABSTRACT: In order to develop a practical method of stability analysis for slopes reinforced by means of steel bars, a series of small model tests using sand were performed with measuring in detail the boundary pressures, tensile reinforcement forces and strain fields in model slopes. The results were analysed by means of the limit equilibrium method. A new method of stability analysis was developed in order to properly deal with inclined boundary forces and reinforcement forces.

1 EXPERIMENTAL METHOD

The sand model slopes (Fig.1) were made up by the air-pluviation method using air dried Toyoura sand and provisions were taken in order to avoid disturbance of the sand around the reinforcements during the placing of sand. The facing consisted of three 1.5 mm thick acrylic plates. The plates were divided vertically with each retaining one third width of the slope surface. After the sand slope together with the reinforcements were set-up the facing plates were fixed to the heads of buried reinforcements by means of miniture screws and epoxy glue. A displacement control system by means of a bellofram cylinder was used for loading the footing. The displacement rate was kept at 0.1 mm/min throughout a test. In order to fail the slope model in such a manner as seen in a prototype slope the loading direction was fixed to 30 degrees from the vertical (see Figs.2~4). A lubricated footing was used in order to avoid the restraint to the lateral displacement of sand by the footing. The footing load was measured at its middle-third to avoid the effect of wall friction by means of eleven two-component small load cells, so that the distribution of normal and shear loads can be obtained. Pictures of the lateral surfaces of model slopes at appropiate displacements of footing were taken so that the displacement and strain fields in the models could be constructed. The coordinates of the targets drawn on the latex membrane used for the side wall lubrication were measured by means of a photogrammetric method, to an accuracy of the order of 20μm.

2 EXPERIMENTAL RESULTS

2.1 Mechanism of failure

The mechanism of failure of the slopes was studied by constructing their strain fields. In the case of unreinforced slope (Fig.2) it was observed that the direction of minor principal strain ε_3 has two distinct tendencies: the one directed horizontally near the heel of footing and the other directed at an angle of approximately 45° to the horizontal in a deeper zone, directed towards the slope surface. Due to this fact it was considered that the best direction of the reinforcement should be such that its direction would be as much as possible in parallel with the tensile strains in deforming zones in the unreinforced slope.

Then, the strain field of reinforced slope without facing (Fig.3) shows that strains in the zone where strains were concentrated in the unreinforced slope were well restrained

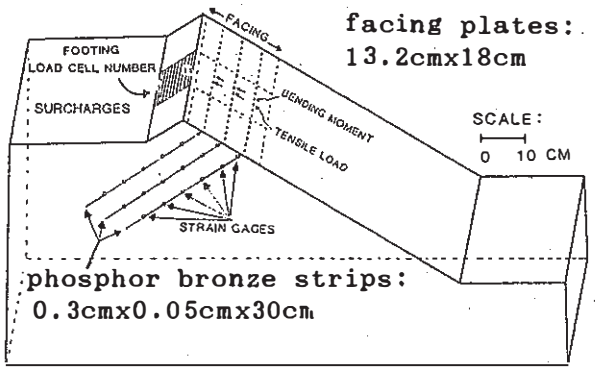

Fig.1 Instrumentation of model slope

by reinforcing, whereas two other failure zones of strain concentration appeared. The first and shallower one was closer to the slope surface and penetrated the reinforced zone. The strength of this reinforced slope seems to have been controlled by this failure. A further development of the first failure was restrained by the reinforcements. A second and deeper failure zone developed and became a clear shear zone. This fact shows

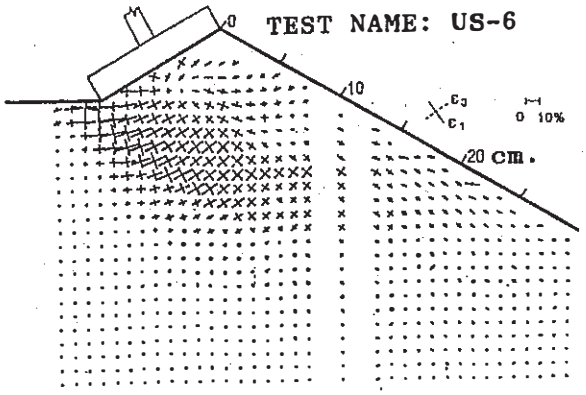

Fig.2 Principal strain distribution of unreinforced slope

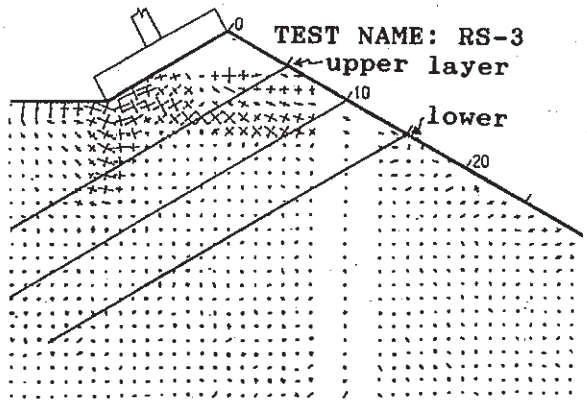

Fig.3 Principal strain distribution of reinforced slope

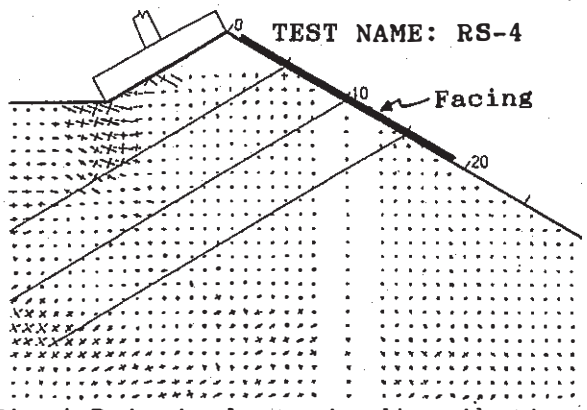

Fig.4 Principal strain distribution of reinforced slope + facing

that the strain field was altered significantly by the reinforcement.

When a facing structure was installed in the reinforced slope (Fig.4) the failure in the shallow zone near the slope surface which appeared in the reinforced slope without facing, was well restrained. At the same time, two zones of strain concentration may be seen; one starts from the heel of footing and passes through the center of the reinforcements and other starts from the lower end of the reinforcements.

2.2 Strength of slopes

The relationships between average axial stress and footing axial displacement for the three model slopes are shown in Fig.5. It may be noticed that despite the increase in the average void ratio of slopes, the strength of slopes increases significantly by means of three layers of metal strips and further by using a facing. After performing several tests with different arrangements of reinforcements and normalizing the results to the same void ratio e=0.69, the effects of facing could be better understood.

Table 1. Condition of reinforcing for each test and rate of increase in axial load.

Test Name	Condition of reinforcing (n=# of strips, l=# of layers)	Rn*
US-6	Unreinforced	—
RS-3	Reinforced without facing (n=54, l=3)	3.2
RS-4	Reinforced with facing (n=54, l=3)	6.9
RS-5	Reinforced with facing (n=54, l=6)	7.5
RS-6	Reinforced with facing (n=27, l=3)	5.3
RS-7	Reinforced with facing (n=9, l=3)	3.6

*The rate of reinforcing Rn was defined for e=0.69 as follows:

$$Rn = \frac{\text{Max footing load of reinforced slope}}{\text{Max footing load of unreinforced slope}} - 1$$

Fig.6 shows the relationship between Rn and the plane density m. This shows a nonlinear pattern. It may be seen that the largest efficiency is obtained at a value of m of around 0.03, which means a light arrangement of reinforcements. The profiles (or distributions) of axial stresses along the length of footing base for the tests listed in Table 1 are shown in Fig.7.

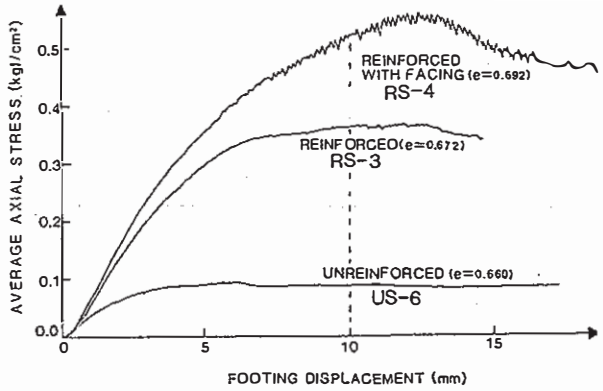

Fig.5 Comparative axial stress-displacement relationships

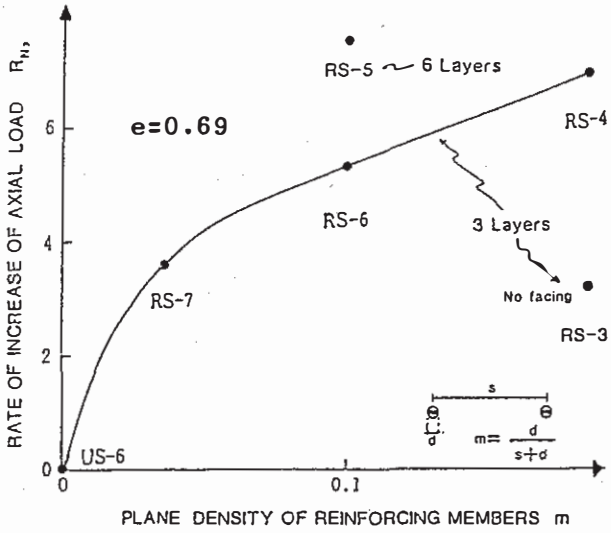

Fig.6 Rate of increase of axial load vs. the plane density

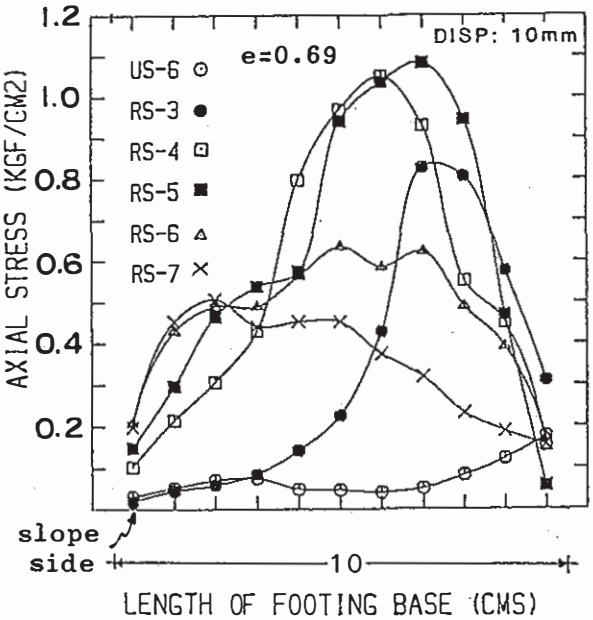

Fig.7 Axial stresses along the length of footing base

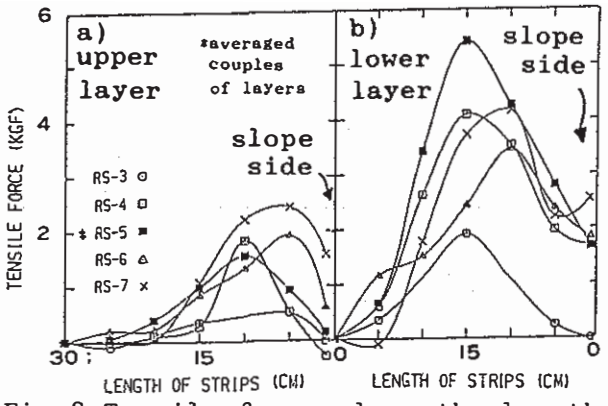

Fig.8 Tensile force along the length of the reinforcements

2.3 Tensile force of reinforcements

The measured forces along the length of strips for a footing displacement of 10mm are shown in Fig.8. This figure can explain the results shown in Fig.7 as follows.

The increase in axial stress and the shifting of its center to the slope surface in Test RS-4 with facing in comparison with Test RS-3 without facing is due to the large increase in tensile force near the slope surface in deep layers (Fig.8b). The enlargement (expansion) of the bell's shape of the axial stresses distribution in Fig.7 from test RS-4 to test RS-5, is due to the increase in tensile reinforcement force attained by a better arrangement of reinforcements (i.e. by increasing the reinforcement layers for the same total number). When the number of reinforcements decreases, the location of the center of axial stresses is shifted towards the slope surface. This corresponds to the increase in tensile force near the slope surface as the number of reinforcements decreases (compare the results by tests RS-4, RS-6, and RS-7 in Fig.8).

3 STABILITY ANALYSIS

3.1 Brief discussion on the Ordinary Method of Slices (Fellenius Method)

In this method, vertically divided slices are employed for all the system of forces acting on the slope regargless of the directions of forces. Thus, when the system of forces in this experimental work (Fig.9) is analysed by the Ordinary Method of Slices (the Fellenius Method), the total normal force ΔFn on the base of each slice is obtained by resolving total forces normal to the base (Chowdbury, 1978), and then, the safety factor for this system is given as:

$$F = \frac{\Sigma\,(W\cos\alpha + P\sin(\beta-\alpha) + T\sin(\gamma+\alpha))\tan\phi}{\Sigma W\sin\alpha + \Sigma P\cos(\beta-\alpha) \pm \Sigma T\cos(\gamma+\alpha)} \qquad (1)$$

where, W=weight of soil in the slice,
P=load of footing working on the top end of slice,
T=tensile force in reinforcement working on the base of slice,
$\Delta F_n \tan\phi$=total shear resistance of soil,
R is the radius of the trial circle, and lw, lp and lt are the arm lengths of those forces.

As can be seen in Eq.(1), the term defining the component of the shear resistance due to the footing load, $P\sin(\beta-\alpha)$, becomes zero when $\beta=\alpha$, and further, when $\beta<\alpha$, it becomes negative. This means that for the same inclination of footing load the shear resistance provided by this component decreases as the angle of slice increases; thus, for the footing pressure on the side of $\beta<\alpha$, for example when a deep failure surface is generated, as in the case where a large degree of reinforcing is used, then the shear resistance decreases with the increase in α, as illustrated in Fig.9b. Of course this situation is not realistic. For the experimental conditions (an inclination angle of footing load of $\beta=60°$ and an inclination angle of reinforcement of $\gamma=30°$) and by using a constant angle of internal friction of sand along the slip line ($\phi=45°$) the safety factor for the observed slip lines shown in Fig.10 were obtained as listed in Table 2.

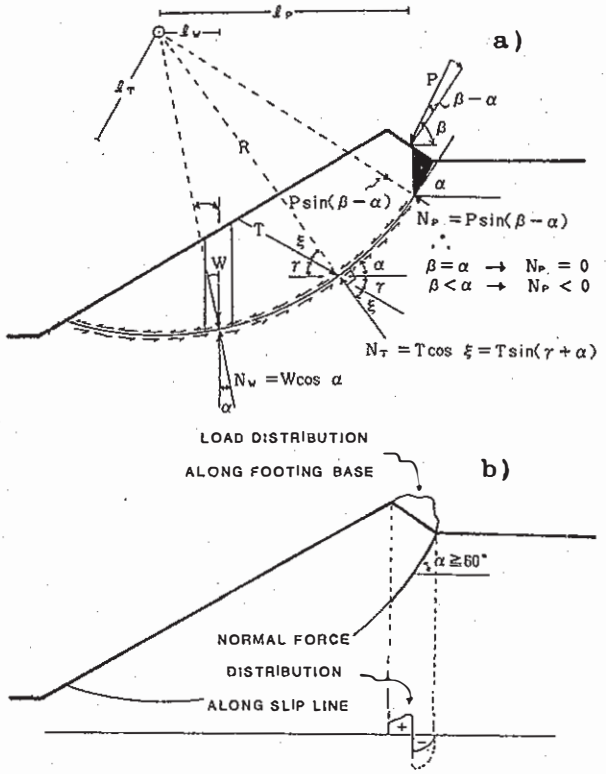

Fig.9 Analysis by Ordinary Method of Slices a) system of forces, b) normal forces along a segment of slip line

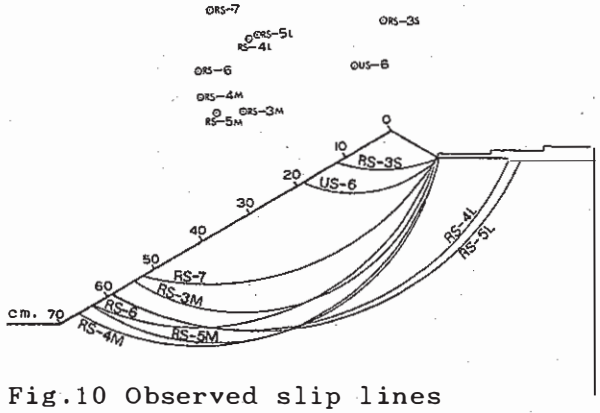

Fig.10 Observed slip lines

Table 2. Results by Ordinary Method of Slices.

Test(slip line)	F
US-6	1.215
RS-3M	0.732
RS-4M	0.693
RS-5M	0.675
RS-6	0.591
RS-7	0.602

These results show that the values of safety factors are underestimated for the reinforced condition considerably. Consequently, in the following, a modification of the direction of slicing is attempted.

3.2 Directional Slicing-Fellenius Method

It was assumed that each load on the surface of the slope acts on the slip line at the point where the line parallel to the direction of the load intersects with the slip line. This is only a generalization of the assumption made for the vertical loads such as the weight of soil or vertical surcharges in the Ordinary Method of Slices. Thus, for each of the forces W,P and T defined before, a different system of slices is produced with keeping the force equilibrium on any slice along the slip line. In each of these systems the normal force on the base of each slice is obtained by resolving total forces normal to the base of slice as in the Ordinary Method of Slices. Considering separately each system of forces working on the slope we have the following:

For the weight of soil, W (Fig.11): only weight of soil is considered; this is the same with the case of an unreinforced slope under gravity forces without exterior loads. In this system the slices are divided vertically, as in the conventional method of slicing.

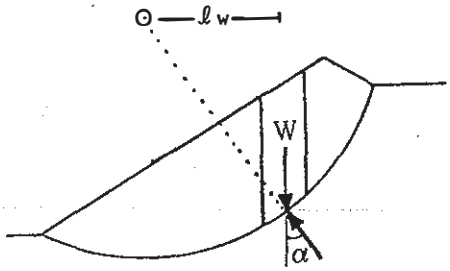

$N_W = W\cos\alpha$

Fig.11 Slicing for weight of soil

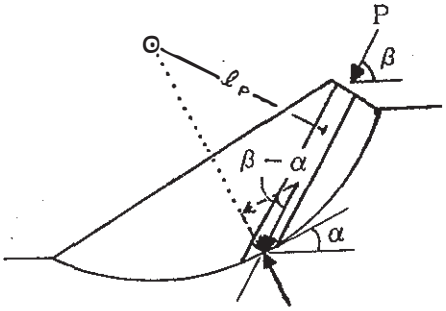

$N_P = P\sin(\beta-\alpha)$

Fig.12 Slicing for footing pressure

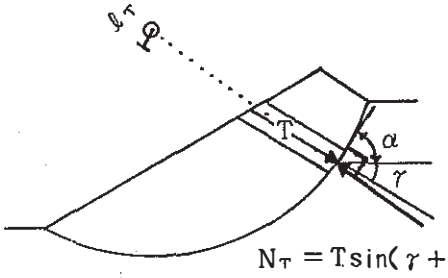

$N_T = T\sin(\gamma+\alpha)$

Fig.13 Slicing for tensile forces

For inclined footing load, P(Fig.12), and inclined tensile reinforcement forces, T (Fig.13): In this systems the slices are divided in the direction of either P or T. Thus, the safety factor for the overall system is obtained by summation of the resistant moments and the driving moments in these different systems. When the subscripts i, j,k are used to distinguish different components for different slices, we obtain the following equation:

$$F=\frac{\Sigma W_i\cos\alpha_i\tan\phi_i+\Sigma P_j\sin(\beta-\alpha_j)\tan\phi_j+\Sigma T_k\sin(\gamma+\alpha_k)\tan\phi_k}{\Sigma W_i\sin\alpha_i+\Sigma P_j l_P/R+\Sigma T_k\cos(\gamma+\alpha_k)} \qquad (2)$$

This is a generalized expression for the directional slicing method by using the specific assumptions of the Fellenius Method. A typical result of the stability analyses performed for an observed slip line when the internal friction angle is considered constant

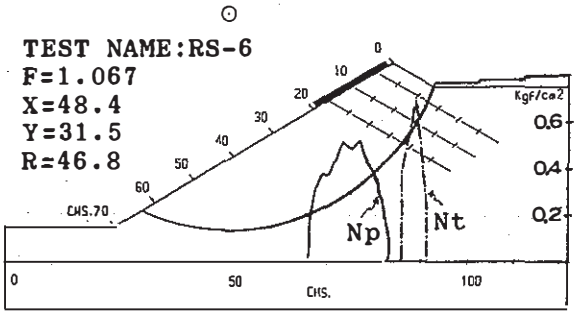

Fig.14 Typical distribution of normal stresses by directional slicing

ϕ=45° is shown in Fig.14. In this figure, Np and Nt are the normal stresses on the slip line due to the footing pressures and the reinforcement forces respectively. This result shows that this proposed method is a more realistic approach as compared with that shown in Fig.9.

In the following analyses, the minimum values of F by Eq.(2) were obtained for the critical circles using the following three kinds of angle of internal friction; 1) a constant value of ϕ=45°, 2) $\phi(\delta)$ with taking into account the strength anisotropy of a model sand (air-pluviated Toyoura sand), i.e., ϕ is a function of δ (the angle of σ_1 direction relative to the bedding plane) with ϕ=45° at δ=90° with the assumption that the σ_1-direction is 45°-ϕ/2 from the direction of failure surface at each point; and 3) $\phi_{mob}(\delta)$ with taking into account further the progressive failure, i.e., the current mobilized angle of friction ϕ_{mob} at each point in the slope is estimated from the measured local values of the shear strain $\gamma_{max}=\varepsilon_1-\varepsilon_3$. In this estimation, the relationships between ϕ_{mob} and γ_{max} in plane strain defined for 1cmx1cm element at e=0.69 as shown in Fig.15 were used. In these relations ϕ=47.7° for δ=90°. Note that ϕ=45° and $\phi(\delta$=90°) are underestimated for the test condition (i.e. e=0.69). A typical result of stability analysis is shown in Fig.16 for test RS-6 in which the contour lines for the shear strain also are shown. It can be observed that an accurate prediction of the critical slip line is obtained by using the actual ϕ_{mob} along the slip line. The summary of the analyses for the unreinforced slope and the slopes reinforced with three layers of reinforcements and facing is shown in Fig.17. In this case, the correct values for safety factors are unity. It may be seen that rather accurate prediction of the safety factor has been obtained.

A rate of the increase in stability by reinforcing may be defined as:

$$Sj=\frac{(FR-FU)}{FU}\times 100 \qquad (3)$$

where FR=the safety factor for the reinforced condition calculated for the critical slip circle in the unreinforced slope, and
FU=minimum safety factor for unreinforced condition.

The rate of increase in stability Si is plotted in Fig.18. An increase in stability as the number of reinforcements increases may be observed. This seems to be a very reasonable result in accordance with the experimental results shown in Fig.6.

Conclusions: It was found that for the system where the inclined reinforcement tensile forces and the inclined footing pressure are incorporated, reasonable values of safety factor and locations of critical slip circles can be obtained only by modifying the Ordinary Method of Slices (Fellenius

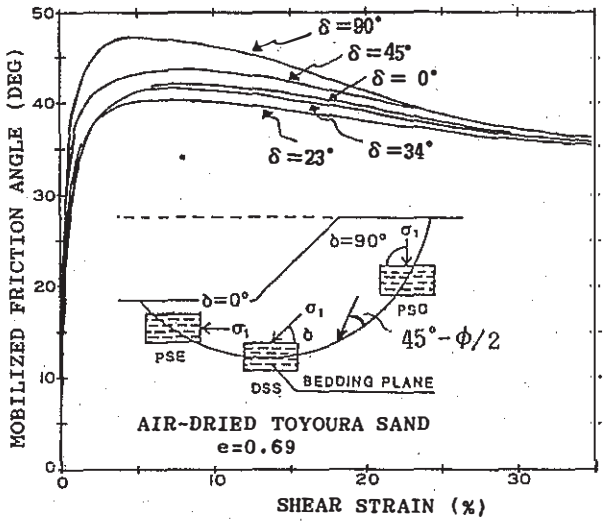

Fig.15 Mobilized friction angle as a function of the shear strain

Condition of Critical Slip Line	safety Factor Fmin
PC: constant φ	1.007
Pd: φ(δ)	0.948
Pm: φmob(δ)	0.951

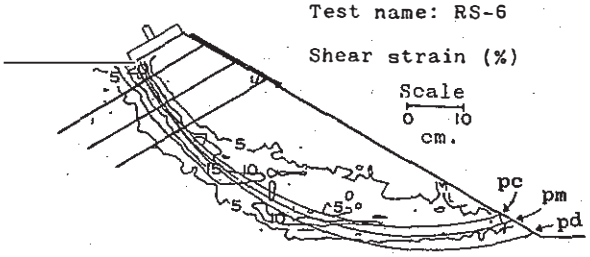

Fig.16 Critical slip lines by Dir. Slicing-Fellenius Method compared with shear strain

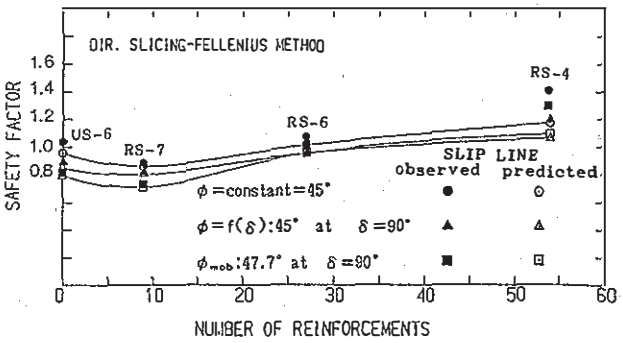

Fig.17 Safety factors vs. number of reinforcements

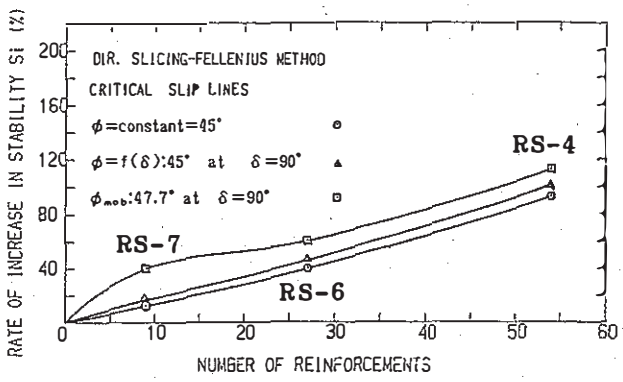

Fig.18 Rate of increase in stability vs. number of reinforcements

Method) into a so called Directional Slicing-Fellenius Method. In order to obtain accurate results using actual properties of soil, the progressive failure should be accounted for. This new method of stability analysis proposed in this work is practical, simple, accurate and versatile.

REFERENCES

Chowdhury, R.N. 1978. Slope analysis; Developments in Geotechnical Engineering, vol.22.

Gutierrez, V. 1988. Sand slopes stabilized with metal reinforcement and facing: model tests and stability analyses. Doctor thesis, University of Tokyo.

Jewell, R.A. 1980. Some effects of reinforcement on the mechanical behavior of soils. Doctor thesis, Cambridge University.

Tatsuoka et all 1986. Strength and deformation characteristics of sand in plane strain at extremely low pressures. Soil and Foundations, 26-1: 65-84. Japan.